

## Reverse Translocation of Nucleotides through a Carbon Nanotube

Mohsen Farshad and Jayendran C. Rasaiah\*

Cite This: <https://dx.doi.org/10.1021/acs.jpcb.9b09587>

Read Online

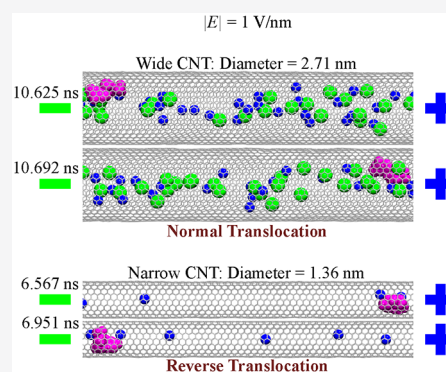
ACCESS |

Metrics &amp; More

Article Recommendations

Supporting Information

**ABSTRACT:** We report molecular dynamics (MD) simulations of the reverse translocation of single nucleotides through a narrow carbon nanotube (CNT), with a diameter of 1.36 nm, immersed in a 1 M KCl electrolyte solution under an applied electric field along the tube axis. We observe ion selectivity by the narrow CNT, which leads to a high flow of  $K^+$  ions, in contrast to a negligible and opposing current of  $Cl^-$  ions. The  $K^+$  ions, driven by the electric field, force a negatively charged single nucleotide into the narrow CNT where it is trapped by the incoming  $K^+$  ions and water molecules, and the nucleotide is driven in the same direction as the  $K^+$  ions. This illustrates a novel mechanism of nucleotide reverse translocation that is controlled by ion selectivity. An increase in the CNT diameter to 2.71 nm or an increase in nucleotide chain length both lead to translocation in the normal direction of the applied field. The reverse translocation rate of single nucleotides is correlated to the ionic current of  $K^+$  ions in the narrow tube, unlike translocation in the normal direction in the wider tube.



## INTRODUCTION

Fundamental studies on ion channels have revealed the subtle mechanisms of ion transport through nanopores and nanochannels.<sup>1–4</sup> Ion channels in the cell membrane facilitate the regulation of ions across the membrane of living cells.<sup>5–10</sup> The normal function of a cell is determined by the precise transport of ions through protein ion channels, which play an important role in the generation of electrical signals and communication between cells.<sup>5–10</sup> The selectivity of ion channels permits specific ions to move spontaneously down a concentration gradient across the membrane and generate an action potential.<sup>5–10</sup> The transport of ions is influenced by their hydrated sizes relative to the diameter of the channel.<sup>11,12</sup> Hydrophobic single-walled carbon nanotubes (CNTs) carry some features that are similar to biological ion channels in nature<sup>13–15</sup> and have been studied to understand the correlation between the channel diameter and selectivity of the channel that is determined by the sizes of hydrated ions and their partial or complete dehydration energies.<sup>14–17</sup> The dehydration of ions, especially  $K^+$  and  $Cl^-$ , as a mechanism for ion selectivity through graphene or atom-sized pores has been recently investigated.<sup>16,17</sup>

Nucleotides,<sup>18–22</sup> along with ions<sup>13–15,23</sup> and water,<sup>24–26</sup> can also be transported through CNTs and other synthetic pores with suitable diameters. It has been suggested that CNTs can be modified to mimic the behavior of biological channels and their selectivity.<sup>15</sup> However, further investigations are necessary to understand the effect of ions on the translocation of nucleotides through nanopores and nanochannels. This is important to understand the behavior of ion pores in membranes and how synthetic channels can be exploited in

nanopore DNA sequencing.<sup>27–29</sup> Clarke et al. drove single nucleotides through an engineered  $\alpha$ -hemolysin nanopore under an applied electric field and identified single nucleotides by measuring the ionic currents and translocation times of nucleotides.<sup>30</sup>

Inspired by their single-nucleotide experiments, we employed all-atom molecular dynamics (MD) simulations to investigate DNA sequencing and the translocation of the single nucleotides adenine (A), guanine (G), cytosine (C), and thymine (T) through CNTs with diameters of 1.36 and 2.71 nm under an applied electric field, with the CNT immersed in a 1 M aqueous electrolyte solution of potassium chloride (KCl).<sup>31–33</sup> The diameter of the CNT is measured as the distance between the centers of carbon atoms at opposite ends. For the small diameter tube, the size of the carbon atoms is comparable to the diameter of the tube. In this regard, the edge-to-edge inner diameters of the narrow and wide CNTs are 1.11 and 2.46 nm, respectively.

During the simulations, we expected that the negatively charged nucleotides, along with  $K^+$  and  $Cl^-$  ions, would translocate through the CNT in the expected directions as determined by their charges and the direction of the external field. However, we encountered an exotic phenomenon in which repeated reverse translocations of a single nucleotide occurred within a narrow CNT with a diameter of 1.36 nm

Received: October 11, 2019

Revised: January 2, 2020

Published: January 9, 2020

under an high applied electric field. An increase in the diameter of the CNT to 2.71 nm or an increase in the length of the nucleotide chain from 1 to 16 led to translocation in the normal direction of the applied field. To the best of our knowledge, the reverse translocation of a nucleotide against the field inside a narrow CNT, which is observed in our all-atom MD simulations, has not yet been reported in the literature. However, an experimental study has shown reverse translocation of DNA under a high applied electric field through a microfluidic channel.<sup>34</sup> To our knowledge, there has also been no detailed explanation of how this occurs at the molecular level.

The direction of nucleotide translocation in a CNT is clearly affected by the diameter of the nanotube relative to the sizes of the ions and the length of the nucleotide chain. The high flow of  $K^+$  ions in comparison to the negligible current of  $Cl^-$  ions through the narrow CNT reverses the translocation direction of a negatively charged single nucleotide. Understanding the impact of ion size, hydration and dehydration energies, and the geometry and distortion of the partially or fully hydrated ions relative to the pore diameter are important to control and detect the transportation of molecules through synthetic and biological pores.

## METHODS

**Molecular Dynamics (MD) Simulations.** To construct the model, we used a VMD package to create the CNT and nucleotide. 3D-DART<sup>35</sup> was used to create the nucleotide which was placed inside the CNT close to the tube entrance (gate). The nucleotide and CNT were immersed in a 1 M KCl ionic solution with 1 g/mL of water. To make the system neutral, we added the required number of  $K^+$  ions, which was always larger than the number of  $Cl^-$  ions, depending on the number of nucleotides present. Each nucleotide carried one negative charge because of the free electron of the oxygen of the phosphate group. The system was created with the VMD<sup>36</sup> graphics package. The simulations were performed, using the NAMD<sup>37</sup> program, with periodic boundary conditions (PBC) at 300 K. These interactions between atoms were implemented in our MD simulation as the sum of the electrostatic Coulombic and Lennard-Jones potentials. The CHARMM27<sup>38</sup> force field with the TIP3P water model was used to implement the interaction between atoms. The size of the largest simulation box (Figure 2a,b) was  $120 \times 140 \times 500 \text{ \AA}^3$ . The time step was 1 fs, and the energy of the system was minimized and equilibrated in an NPT ensemble without an electric field, and the pressure was set to 1 atm. Then the system was equilibrated in an NVT ensemble under an applied electric field. To keep the CNT at the center of the reservoir, we allowed each carbon of the CNT to only oscillate harmonically about its center. To avoid translocation of a nucleotide during the minimization and equilibration, we anchored one atom of the nucleotide with a harmonic potential such that the nucleotide could fluctuate around the center of the fixed atom.

The PBC in our simulations implemented an infinite number of CNTs and reservoirs next to each other. To save on computing time, except for one large system presented in Figure 2a,b, we kept the reservoir small for all systems to the extent that the CNTs did not interact with each other appreciably, and there was always only one CNT close to a nucleotide. This increased the probability of nucleotide absorption on the surface of the CNT because of attractive forces between the CNT and nucleotide. Therefore, a

nucleotide could translocate in the reservoir along the surface of the CNT in the direction of the electric field. Once the nucleotide reached the end of the CNT, in some cases, it turned back toward the entrance of the CNT and finally entered the CNT to translocate in the reverse direction. In other cases, the nucleotide left the CNT and continued to move in the normal direction of the electric field. Outside the CNT, the nucleotide was always transported in the direction of the field.

**Electric Ionic Current.** Equation 1 was used to calculate the electric current from the MD trajectories:

$$I(t) = \frac{1}{l_z \Delta t} \sum_{i=1}^N q_i [z_i(t + \Delta t) - z_i(t)] \quad (1)$$

where  $q_i$  is the charge of ion  $i$  and  $l_z$  is the length of CNT. The charges of  $Cl^-$  and  $K^+$  are  $-1$  or  $+1$ , respectively.  $z_i(t)$  is the  $z$  coordinate of ion  $i$  at time  $t$ , and  $z_i(t + \Delta t)$  is the  $z$  coordinate of ion  $i$  at time  $t + \Delta t$ . The difference between  $z_i(t + \Delta t)$  and  $z_i(t)$  is the distance that ion  $i$  moves in the direction of  $z$  in the time frame step  $\Delta t$  of the MD simulations, which was 1 ps. The ionic currents contained large fluctuations (Figure 2c,d) because of the high sampling frequency of  $10^{12} \text{ s}^{-1}$ . Consequently, we filtered the data to increase the signal resolution. We used the moving average filter function in MATLAB to smooth out the fluctuations.

## RESULTS AND DISCUSSION

Figure 1 demonstrates the general scheme of our CNT immersed in an ionic solution under an applied electric field.

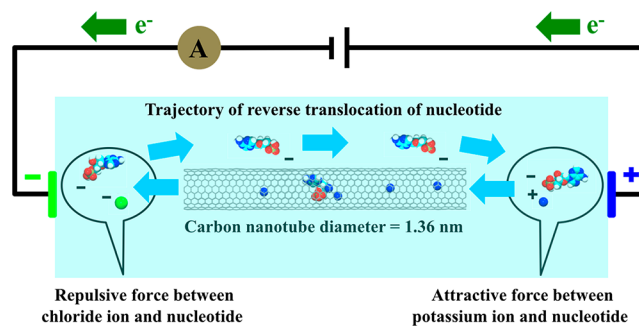


**Figure 1.** General scheme of the system. The reservoir (transparent blue) is connected to the electric field along the  $z$ -axis. The blue and green spheres are  $K^+$  and  $Cl^-$  ions. The gray cylinder represents the CNT with a diameter of 1.36 nm (inner diameter of 1.11 nm) in an aqueous reservoir of 1 M KCl. The cyan arrows show the trajectory of a single adenine nucleotide under an applied electric field in the normal direction outside the CNT and in the reverse direction inside the CNT. The green arrows show the direction of electron flow. The water molecules are not represented.

This illustrates the passage of the nucleotide first outside and along the length of the CNT followed by reverse translocation through the CNT.

Figure 1 schematically shows how the attractive ( $K^+$  with a single nucleotide) and repulsive ( $Cl^-$  with a single nucleotide) forces between the nucleotide and the ions facilitated nucleotide transport through the CNT under an external voltage bias.

Our MD simulations showed that a negatively charged single nucleotide in a 1 M KCl solution rarely entered the narrow 1.36 nm diameter CNT from the expected direction of the

applied electric field of 1 V/nm, but moved along the outside wall of the tube, and unpredictably entered the tube from the other gate of the CNT to be translocated rapidly in the reverse direction of the field. However, the negatively charged nucleotide traversed through the tube in the normal direction of the electric field when the diameter of the CNT was increased to 2.71 nm or more in the 1 M KCl ionic solution. Figure 2a–e demonstrates the reverse translocation of a single

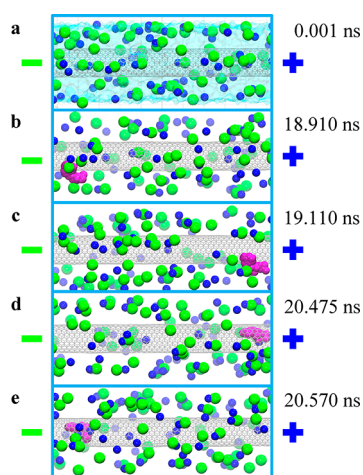


**Figure 2.** Schematic illustrations of the translocation of a single adenine nucleotide in a 1 M KCl solution containing a 50 nm long CNT with a diameter of 1.36 nm over time (ns). (a) An image of the system after equilibration. The nucleotide has not arrived to this part of the system as yet. (b, c) Normal translocation of adenine through the reservoir along the outside wall of the CNT with a diameter of 1.36 nm in 0.2 ns, followed by (d, e) reverse translocation through the same CNT in 0.095 ns. All images are representations of the  $\sim 10.2$  nm  $\times$   $\sim 4$  nm systems. The green and blue spheres are  $\text{Cl}^-$  and  $\text{K}^+$  ions, respectively, and the gray cylinder is the CNT. The adenine is colored purple. The water molecules are not shown in b–e.

adenine nucleotide inside a 1.36 nm diameter nanotube and normal translocation outside the CNT at different times. We observed that the reverse translocation of the nucleotide inside the narrow CNT was faster than the translocation of the nucleotide in the normal direction of the field along the outside wall of the CNT in the reservoir (Figure 2b–e).

To understand the reverse translocation of a nucleotide inside the narrow CNT, we hypothesized that the ion selectivity of the narrow tube, spatial restrictions, and relative forces of  $\text{K}^+$  and  $\text{Cl}^-$  ions on the nucleotide inside the narrow CNT in the presence of the electric field were the causes of reverse translocation. In a narrow CNT, it becomes harder for the larger hydrated  $\text{Cl}^-$  ions to enter the CNT<sup>15</sup> compared with the smaller  $\text{K}^+$  ions because there is a high energy barrier for ions to enter the pore due to their hydration shells and the size of the pore.<sup>39,40</sup>

Steric hindrance of the nanopore is very sensitive to the size of the pore relative to the size of hydrated ions, and consequently small changes in diameter of pore or size of ions make a significant difference in ion selectivity of the pore.<sup>41,42</sup> This problem has been studied extensively by Liu, Jameson, and Murad.<sup>43</sup> While the coordination numbers of  $\text{Cl}^-$  and  $\text{K}^+$  ions inside the tube are 6.14 and 6.69, respectively, the coordination numbers for the same ions outside the tube are 6.38 and 7.28, respectively. The coordination numbers of  $\text{Cl}^-$  and  $\text{K}^+$  ions inside the tube are slightly smaller than when they

are outside the tube. This implies ions that are partially dehydrated can enter the CNT. Furthermore, comparison of the maximum and minimum of the first solvation shell of ions (Supporting Information Figure S1) shows distortion in the arrangement of the water molecules around the ions inside the tube. Water molecules around ions may rearrange to minimize the steric hindrance of the pore.

Partial or complete dehydration of ions is necessary for ions to be transported through the narrow pore.<sup>16,17</sup> The diameter of a hydrated ion shell and its dehydration energy varies among different ions.<sup>44</sup> Dehydration of  $\text{Cl}^-$  ions requires a higher energy expenditure than the dehydration of  $\text{K}^+$  ions.<sup>16,17,45</sup> The lower dehydration energy,<sup>45</sup> higher mobility,<sup>46,47</sup> and smaller size<sup>48</sup> of the hydrated  $\text{K}^+$  ions, compared with the hydrated  $\text{Cl}^-$  ions (Figure S1a,b), are the factors that drive substantially more  $\text{K}^+$  ions than  $\text{Cl}^-$  ions through a narrow CNT in an applied field.

The smaller  $\text{K}^+$  ions entering the CNT cannot easily move around, or pass by negatively charged nucleotide in the narrow CNT, because of the restricted space and the attractive forces between them (Figure S2). As a result, the nucleotide is forced to move in the reverse direction under an applied field. The ionic force on a nucleotide from  $\text{K}^+$  ions traversing in the normal direction through the narrow tube under an electric field pushes the negatively charged nucleotide trapped within the tube in the reverse direction, which overcomes the electromagnetic force of the electric field on single nucleotide during reverse translocation. However, when the CNT diameter is large, both  $\text{Cl}^-$  and  $\text{K}^+$  ions are present in the tube and apply forces on the nucleotide in the direction dictated by their attraction to or repulsion from the negatively charged nucleotide, and the nucleotide moves in the normal direction determined by the external field.

We tested this hypothesis by measuring the individual ionic currents of  $\text{K}^+$  and  $\text{Cl}^-$  ions through CNTs diameters of 1.36 and 2.71 nm. The ionic net force was typically less than the applied electric force on a chain of 16 nucleotides carrying 15 negative charges from the phosphate groups, and the chain moved in the normal direction of the field. Figure 3a,b shows axial and lateral perspectives of an equilibrated system, and Figure 3c,d displays the individual currents of  $\text{K}^+$ ,  $\text{Cl}^-$ , and the total current of KCl through a CNT with a diameter of 1.36 nm immersed in a reservoir of 1 M KCl. It is obvious that the  $\text{Cl}^-$  ion current is negligible in comparison to the  $\text{K}^+$  ion current with ion selectivity of  $I_{\text{K}^+}/I_{\text{Cl}^-} = 39.10$  on average in this system. Figure 3e shows the individual and total cumulative charge transfers illustrating the selectivity of the narrow CNT.

The system shown in Figure 3a,b represents the largest one tested in our simulations to observe the translocation of nucleotides. It consisted of a CNT with a length of 20 nm and a diameter of 1.36 nm immersed in a 1 M KCl solution with 144914 water molecules, 2611 potassium ions, 2610 chloride ions, and a single negatively charged nucleotide. An electric field of 1 V/nm was applied across the system in the axial  $z$ -direction of the CNT. The adenine rarely entered the CNT in the direction of the electric field and traversed outside along the wall of the CNT. When the negatively charged nucleotide reached the opposite gate, it was forced into the CNT by the hydrated  $\text{K}^+$  ions outside the gate to which it was attracted and moved in the reverse direction. The capture of the nucleotide into the tube was also aided by the nucleotide–CNT attractive force. The nucleotide traversed through the CNT in the reverse direction until it exited from the other gate and moved

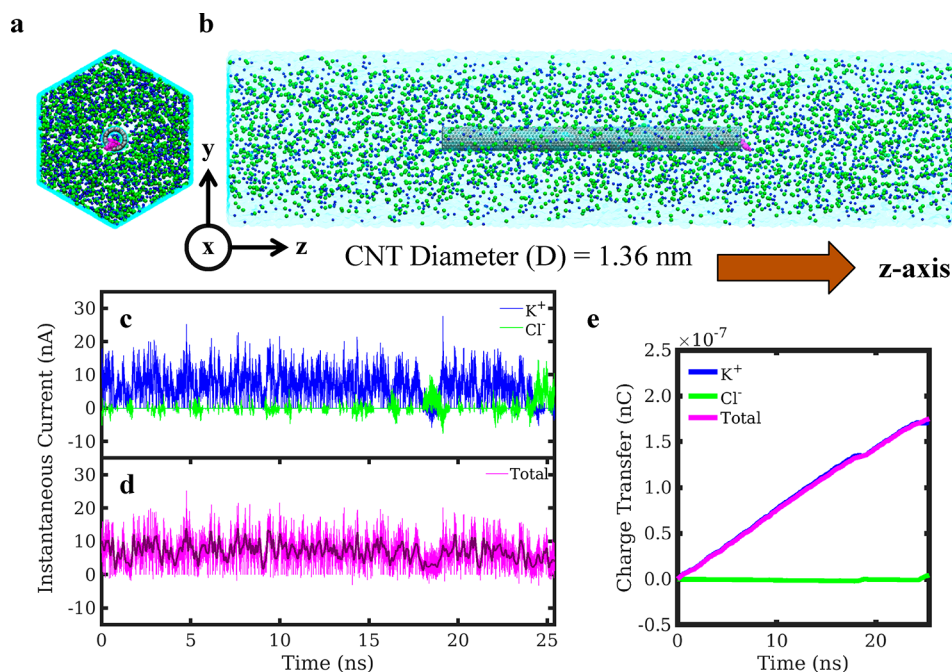


**Figure 3.** Ionic currents through a CNT with a diameter of 1.36 nm and a length of 20 nm under an applied electric field of 1 V/nm. (a, b) Schematic perspective of the system along the  $z$ - and  $x$ -axes, respectively. Green and blue spheres represent the  $\text{Cl}^-$  and  $\text{K}^+$  ions, respectively. The gray cylinder is the CNT, the cyan continuum color is the water reservoir, and the purple molecule next to the CNT gate is a nucleotide. (c) Individual ionic currents of 1 M  $\text{K}^+$  and  $\text{Cl}^-$  ions are represented by the blue and green lines, respectively. (d) The pink line is the total averaged current, and (e) shows the charge transfers of  $\text{K}^+$  and  $\text{Cl}^-$  ions.

again in the normal direction outside the CNT next to the wall in the reservoir. We repeatedly observed reverse translocation of the adenine nucleotide through the CNT. Furthermore, the negative current of  $\text{Cl}^-$  ions indicated that the  $\text{K}^+$  ions carried them occasionally as pairs<sup>49</sup> ( $\text{KCl}$ ) in the reverse direction through the narrow CNT against the strong external field. The reverse translocation was also observed for the G, T, and C single nucleotides.

On increasing the diameter of the CNT from 1.36 to 2.71 nm, we found that the negatively charged nucleotide moved in the direction of the electric field. The image of the system during the translocation of adenine through the narrow CNT in Figure 4a confirmed the presence of potassium ions that translocated through the CNT along with the nucleotide and occasionally a paired chloride ion present inside the CNT.<sup>49</sup> In this case, the ionic current ratio of  $I_{\text{K}^+}/I_{\text{Cl}^-} = -29.20$  through the narrow CNT of length of 50 nm was negative under 1 V/nm applied electric field as the  $\text{Cl}^-$  ions translocated in the reverse direction paired with potassium ions. In the wide CNT of length of 20 nm under 1 V/nm applied electric field, the ionic current ratio was  $I_{\text{K}^+}/I_{\text{Cl}^-} = 0.98$ . The corresponding image in Figure 4b shows an almost equal number of potassium and chloride ions translocating along with the negatively charged nucleotide through the larger diameter CNT in their normal directions under an applied electric field. Figure 4c presents the accumulated charge transfer of  $\text{K}^+$ ,  $\text{Cl}^-$ , and the total current through the narrow CNT, which was completely dominated by the  $\text{K}^+$  ions. Conversely, Figure 4d shows an approximately equal flow of  $\text{K}^+$  and  $\text{Cl}^-$  ions moving in opposite directions through the wider CNT. Ion selectivity was absent in the wider nanotube. A video of reverse translocation of an adenine nucleotide through a narrow CNT with a diameter of 1.36 nm under an electric field of 1 V/nm is provided in the Supporting Information.

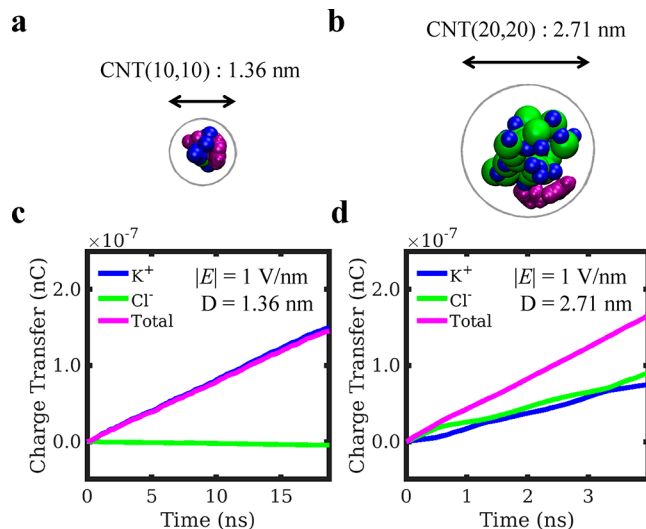


**Figure 4.** Ionic currents through two sizes of CNTs. (a, b) A perspective of CNTs (gray circles) along the tube axis showing the adenine nucleotide,  $\text{K}^+$ , and  $\text{Cl}^-$  ions represented by purple, blue, and green colors, respectively, inside the CNTs. (c, d) Comparison of the charge transfers of  $\text{K}^+$  and  $\text{Cl}^-$  ions and the total current through the narrow (1.36 nm) and wide (2.71 nm) CNTs. Ion selectivity is absent in the wider nanotube.

The CNT–nucleotide,<sup>50,51</sup> ion–nucleotide,<sup>52</sup> and water–nucleotide<sup>53</sup> interactions affect the translocation rate of nucleotides inside nanopores and nanotubes. To investigate the correlation between the flow of  $\text{K}^+$  ions and the translocation rates of nucleotides A, G, T, and C through the CNT, we plotted the average ionic current (nA) against the translocation rates (m/s) in Figure 5a,b. For the narrow CNT (Figure 5a), the translocation was in the reverse

direction, whereas it was in the normal direction (Figure 5b) for the wide CNT.

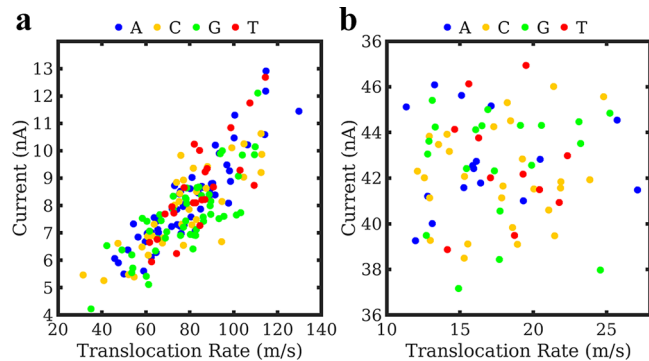


**Figure 5.** Two-dimensional diagram of average ionic currents (nA) and translocation rates (m/s) of nucleotides (A, G, T, and C) during reverse and normal translocations, respectively, through CNTs (a) with a diameter of 1.36 nm and length of 50 nm and (b) with a diameter of 2.71 nm and length of 20 nm, under an applied voltage of 1 V/nm.

Figure 5a indicates an approximately linear correlation between the reverse translocation rate of the nucleotide and average ionic current through the narrow CNT with a diameter of 1.36 nm under an applied electric field of 1 V/nm. Figure 5b does not indicate a clear correlation between the normal translocation rate of a nucleotide and the average ionic current through the wider CNT with a diameter of 2.71 nm. This suggested that the reverse translocation rate of a nucleotide inside a narrow CNT was correlated to the ionic current which resulted from the close interaction between  $K^+$  and a single nucleotide in the narrow CNT. Single nucleotides were forced in the reverse direction by the strong current of  $K^+$  ions in the narrow CNT, whereas  $Cl^-$  ions rarely entered the CNT and contributed weakly to the current. The  $K^+$  ions move faster than nucleotides because of their higher charge to mass ratio in comparison to nucleotides. In this regard, the nucleotide inside the tube is carried faster in the reverse direction inside the CNT than the normal translocation of nucleotide outside the CNT.

The reverse translocation of adenine nucleotide inside the CNT was also observed at lower electric fields of  $\sim 0.17$  and  $\sim 0.35$  V/nm. We calculated the translocation rates of adenine nucleotide in the reverse direction inside the CNT and in the normal direction outside the CNT. The results show that the translocation rate in both cases decreases with a decrease in voltage from 1 to  $\sim 0.17$  V/nm. Within this range, the decrease with the electric field is almost linear inside the CNT. Figure 6a also shows that the average translocation rate of the nucleotide inside the CNT decreases faster than translocation rate outside the CNT which is in the opposite direction.

The trends in Figure 6a imply that the translocation rate of adenine nucleotide inside and outside the CNT are near the intersection below a voltage of  $\sim 0.17$  V/nm and near zero at a lower voltage. A simulation at an applied electric field of  $\sim 0.017$  V/nm of more than 200 ns showed a fluctuating nucleotide moving back and forth inside the narrow CNT. This indicates the adenine nucleotide resists motion in the direction of electric field inside the CNT due to forces applied on the nucleotide from the flow of  $K^+$  ions and water. However, these forces are not enough for reverse translocation

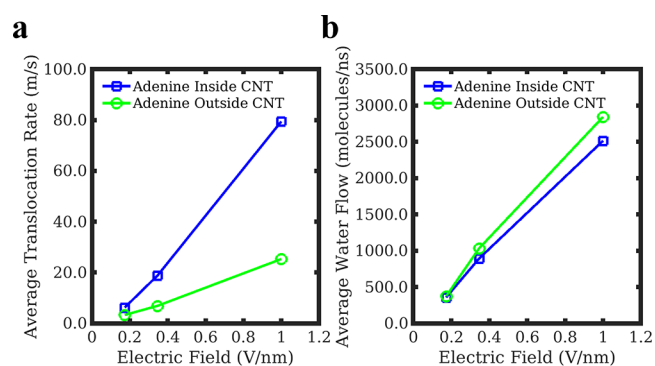


**Figure 6.** (a) Average translocation rate (m/s) of adenine nucleotide and (b) average flow rate of water inside and outside the CNT with a diameter of 1.36 nm (i.d. 1.11 nm) and length of 50 nm under applied voltages of  $\sim 0.17$ ,  $\sim 0.35$ , and 1 V/nm. The translocation of adenine nucleotide is against the field inside the CNT and in the direction of the field outside the CNT. The average water flow inside the tube is in the same direction when the nucleotide is inside and outside the tube. The translocation rate is in the opposite direction when nucleotide is inside and outside the tube.

to occur within the short 200 ns MD time frame at the lower voltage of  $\sim 0.017$  V/nm. This suggests that the direct force on the nucleotide in the direction of the electric field is matched by the force on the nucleotide by the  $K^+$  ion and water carried in the opposite direction at this field. The nucleotide moves in the normal direction outside the CNT under low applied voltages. To further understand the role of water and electroosmotic effect on reverse translocation, we calculated the flow of water through the CNT when nucleotide was inside and outside the tube as shown in Figure 6b and discussed below.

We calculated the flow of water through the CNT when the nucleotide was inside and outside the tube. Figure 6b shows that the average flow rate of water when the nucleotide was inside the tube is less than the average flow rate when the nucleotide was outside the tube. The presence of the nucleotide inside the tube decreases the average flow rate of water through the narrow CNT and partially blocks the passage of water molecules, indicating the electroosmotic effect on reverse translocation. The cumulative water flow shown in Figures S3–S5 similarly shows higher flow rates of water when the nucleotide was outside than when it was inside the tube under different voltages. Moreover, the cumulative flow of water through the wider CNT (Figure S6) is in the opposite direction of the flow of water molecules through the narrow CNT.

The narrow tube is selective to  $K^+$  ions while both  $K^+$  and  $Cl^-$  ions are transported in opposite directions through the wider CNT when the nucleotide translocates in the normal direction through CNT as required by the electric field. The flow of water is associated with the transport of hydrated ions through the wide and narrow tubes. Therefore, electroosmotic flow driven by the hydrated or partially hydrated ions is also effective in nucleotide translocation through CNT.

The tube is filled with water before the ions enter, and the partially hydrated ions assist in pushing the water into and through the tube.<sup>54</sup> Apparently, water does play an important role in moving nucleotides in reverse translocation; however, the fundamental driving force in the system comes from ions under an applied field.

The concept of a net ionic force on nucleotide translocation in an electric field can be applied to the transport of macromolecules through nanopores and nanochannels by varying the pore width, the magnitude of voltage pulses, and ion types. Single nucleotide translocation through synthetic and biological nanopores can be exploited further in nanopore DNA sequencing.<sup>29,55</sup>

We studied reverse translocation in the presence of a membrane around the middle of the CNT to mimic a biological nanopore (Figure S7). The reverse movements of nucleotide are observed in this system; however, the accumulation of ions next to the membrane resisted reverse translocation of nucleotide. The translocation of nucleotide through membranes should be investigated further to find the optimum condition under which reverse translocation is facilitated.

Previous MD simulations indicate that the translocation of DNA through a nanopore is influenced by the size of the ions and magnitude of the electric field.<sup>52,53</sup> A smaller cation will result in a slower translocation of DNA through the nanopores with diameters of 15–20 nm.<sup>52</sup> Aksimentiev et al. used MD simulations to observe that DNA is prevented from entering a narrow nanopore under higher voltage biases.<sup>53</sup> By increasing the voltage bias from 0.1 to 0.2 V, the capture rate of DNA into a nanopore with a diameter of 3.5 nm increased by a factor of 2 and decreased to zero as the voltage was increased further from 0.2 to 1 V.<sup>53</sup> The hydrated ions in addition to DNA are the only charged species in the system and play an important role in the flow of water and translocation of DNA through the nanopore.

## CONCLUSIONS

In conclusion, our study provides a unified fundamental concept to understand the transport phenomena through synthetic and biological nanopores of different diameters that discriminate between ions in solution. Narrow nanopores and nanochannels are selective to certain ions depending on the ion sizes and the dehydration energy barriers. The principle of the reverse and normal translocation modes of nucleotides is investigated and is shown to be related to the selectivity of narrow nanopores to the passage of ions. In particular, the selectivity of narrow nanopores to the  $K^+$  ion over a  $Cl^-$  ion, and the attraction between  $K^+$  and negatively charged single nucleotides is the cause of the reverse translocation of nucleotides through narrow pores in the presence of an electric field. Our simulations show that nucleotides can be driven through narrow pores in a direction counter to an applied electric field aided by the ion selectivity of the pore.

## ASSOCIATED CONTENT

### Supporting Information

The Supporting Information is available free of charge at <https://pubs.acs.org/doi/10.1021/acs.jpcc.9b09587>.

Calculation and description of radial distribution functions of ions around water and ions around the adenine nucleotide. Water flow calculations. A description of a system with a graphene sheet as membrane near the middle of the CNT (PDF)

Reverse translocation of a single adenine nucleotide through 1.36 nm CNT (MP4)

## AUTHOR INFORMATION

### Corresponding Author

Jayendran C. Rasaiah – Department of Chemistry, University of Maine, Orono, Maine 04469, United States; [orcid.org/](https://orcid.org/) 0000-0002-4453-7438; Phone: +1 3017680175; Email: [rasaiah@maine.edu](mailto:rasaiah@maine.edu)

### Author

Mohsen Farshad – Department of Chemistry, University of Maine, Orono, Maine 04469, United States; [orcid.org/](https://orcid.org/) 0000-0001-5095-4361

Complete contact information is available at: <https://pubs.acs.org/10.1021/acs.jpcc.9b09587>

### Notes

The authors declare no competing financial interest.

## ACKNOWLEDGMENTS

We thank Dylan Suvlu for his assistance in writing scripts for the calculation of ionic currents. We also thank Iranga Subasinghe from the School of Computing and Information Science at the University of Maine for his programming assistance. We thank the Advanced Computing Group of the University of Maine for providing us with computer time, specifically Stephen Cousins, who assisted us with using their computing systems. We thank the Edanz Group for editing a draft of this manuscript.

## REFERENCES

- (1) Dixon, J. E.; Shi, W.; Wang, H.-S.; McDonald, C.; Yu, H.; Wymore, R. S.; Cohen, I. S.; McKinnon, D. Role of the Kv4.3 K<sup>+</sup> Channel in Ventricular Muscle. *Circ. Res.* **1996**, *79* (4), 659–668.
- (2) Gutman, G. A.; Chandy, K. G.; Grissmer, S.; Lazdunski, M.; McKinnon, D.; Pardo, L. A.; Robertson, G. A.; Rudy, B.; Sanguinetti, M. C.; Stühmer, W.; et al. International Union of Pharmacology. LIII. Nomenclature and Molecular Relationships of Voltage-Gated Potassium Channels. *Pharmacol. Rev.* **2005**, *57* (4), 473–508.
- (3) Wang, H. S.; Pan, Z.; Shi, W.; Brown, B. S.; Wymore, R. S.; Cohen, I. S.; Dixon, J. E.; McKinnon, D. KCNQ2 And KCNQ3 Potassium Channel Subunits: Molecular Correlates of the M-Channel. *Science* **1998**, *282* (5395), 1890–1893.
- (4) Varma, S.; Rogers, D. M.; Pratt, L. R.; Rempe, S. B. Design Principles for K Selectivity in Membrane Transport. *J. Gen. Physiol.* **2011**, *137* (6), 479–488.
- (5) Hille, B. *Ion Channels of Excitable Membranes*; Sinauer: Sunderland, MA, 2001.
- (6) Neverisky, D. L.; Abbott, G. W. Ion Channel–Transporter Interactions. *Crit. Rev. Biochem. Mol. Biol.* **2016**, *51* (4), 257–267.
- (7) Corry, B. Understanding Ion Channel Selectivity and Gating and Their Role in Cellular Signalling. *Mol. BioSyst.* **2006**, *2* (11), 527.
- (8) Maffeo, C.; Bhattacharya, S.; Yoo, J.; Wells, D.; Aksimentiev, A. Modeling and Simulation of Ion Channels. *Chem. Rev.* **2012**, *112* (12), 6250–6284.
- (9) Capener, C. E.; Kim, H. J.; Arinaminpathy, Y.; Sansom, M. S. Ion channels: Structural Bioinformatics and Modeling. *Hum. Mol. Genet.* **2002**, *11* (20), 2425–2433.
- (10) Roux, B. Ion Channels and Ion Selectivity. *Essays Biochem.* **2017**, *61* (2), 201–209.
- (11) Esfandiari, A.; Radha, B.; Wang, F. C.; Yang, Q.; Hu, S.; Garaj, S.; Nair, R. R.; Geim, A. K.; Gopinadhan, K. Size Effect in Ion Transport through Angstrom-Scale Slits. *Science* **2017**, *358* (6362), 511–513.
- (12) Rigo, E.; Dong, Z.; Park, J. H.; Kennedy, E.; Hokmabadi, M.; Almonte-Garcia, L.; Ding, L.; Aluru, N.; Timp, G. Measurements of the Size and Correlations between Ions Using an Electrolytic Point Contact. *Nat. Commun.* **2019**, *10* (1), 2382.

- (13) Yu, M.; Funke, H. H.; Falconer, J. L.; Noble, R. D. Gated Ion Transport Through Dense Carbon Nanotube Membranes. *J. Am. Chem. Soc.* **2010**, *132* (24), 8285–8290.
- (14) Choi, W.; Ulissi, Z. W.; Shimizu, S. F.; Bellisario, D. O.; Ellison, M. D.; Strano, M. S. Diameter-Dependent Ion Transport Through the Interior of Isolated Single-Walled Carbon Nanotubes. *Nat. Commun.* **2013**, *4* (1), 2397.
- (15) Amiri, H.; Shepard, K. L.; Nuckolls, C.; Sánchez, R. H. Single-Walled Carbon Nanotubes: Mimics of Biological Ion Channels. *Nano Lett.* **2017**, *17* (2), 1204–1211.
- (16) Sahu, S.; Di Ventra, M.; Zwolak, M. Dehydration as a Universal Mechanism for Ion Selectivity in Graphene and Other Atomically Thin Pores. *Nano Lett.* **2017**, *17* (8), 4719–4724.
- (17) Sahu, S.; Zwolak, M. Ionic Selectivity and Filtration from Fragmented Dehydration in Multilayer Graphene Nanopores. *Nanoscale* **2017**, *9* (32), 11424–11428.
- (18) Ito, T.; Sun, L.; Crooks, R. M. Electrochemical Etching of Individual Multiwall Carbon Nanotubes. *Electrochem. Solid-State Lett.* **2003**, *6* (1), C4.
- (19) Yeh, I.-C.; Hummer, G. Nucleic Acid Transport Through Carbon Nanotube Membranes. *Proc. Natl. Acad. Sci. U. S. A.* **2004**, *101* (33), 12177–12182.
- (20) Gao, H.; Kong, Y.; Cui, D.; Ozkan, C. S. Spontaneous Insertion of DNA Oligonucleotides into Carbon Nanotubes. *Nano Lett.* **2003**, *3* (4), 471–473.
- (21) Pei, Q. X.; Lim, C. G.; Cheng, Y.; Gao, H. Molecular Dynamics Study on DNA Oligonucleotide Translocation Through Carbon Nanotubes. *J. Chem. Phys.* **2008**, *129* (12), 125101.
- (22) Liu, H.; He, J.; Tang, J.; Liu, H.; Pang, P.; Cao, D.; Krstic, P.; Joseph, S.; Lindsay, S.; Nuckolls, C. Translocation of Single-Stranded DNA Through Single-Walled Carbon Nanotubes. *Science* **2010**, *327* (5961), 64–67.
- (23) Joseph, S.; Mashl, R. J.; Jakobsson, E.; Aluru, N. R. Electrolytic Transport in Modified Carbon Nanotubes. *Nano Lett.* **2003**, *3* (10), 1399–1403.
- (24) Hummer, G.; Rasaiah, J. C.; Noworyta, J. P. Water Conduction Through the Hydrophobic Channel of a Carbon Nanotube. *Nature* **2001**, *414* (6860), 188–190.
- (25) Majumder, M.; Chopra, N.; Andrews, R.; Hinds, B. J. Nanoscale Hydrodynamics: Enhanced Flow in Carbon Nanotubes. *Nature* **2005**, *438* (7064), 44–44.
- (26) Holt, J. K.; Park, H. G.; Wang, Y.; Stadermann, M.; Artyukhin, A. B.; Grigoriopoulos, C. P.; Noy, A.; Bakajin, O. Fast Mass Transport Through Sub-2-Nanometer Carbon Nanotubes. *Science* **2006**, *312* (5776), 1034–1037.
- (27) Jain, M.; Koren, S.; Quick, J.; Rand, A.; Sasani, T.; Tyson, J.; Beggs, A.; Dilthey, A.; Fiddes, I.; Malla, S.; et al. Nanopore Sequencing and Assembly of a Human Genome with Ultra-Long Reads. *Nat. Biotechnol.* **2018**, *36*, 338–345.
- (28) Kasianowicz, J. J.; Brandin, E.; Branton, D.; Deamer, D. W. Characterization of Individual Polynucleotide Molecules Using a Membrane Channel. *Proc. Natl. Acad. Sci. U. S. A.* **1996**, *93* (24), 13770–13773.
- (29) Branton, D.; Deamer, D. W. *Nanopore Sequencing: An Introduction*; World Scientific Publishing Co. Pte. Ltd.: 2019.
- (30) Clarke, J.; Wu, H.-C.; Jayasinghe, L.; Patel, A.; Reid, S.; Bayley, H. Continuous Base Identification for Single-Molecule Nanopore DNA Sequencing. *Nat. Nanotechnol.* **2009**, *4* (4), 265–270.
- (31) He, J.; Liu, H.; Pang, P.; Cao, D.; Lindsay, S. Translocation Events in a Single-Walled Carbon Nanotube. *J. Phys.: Condens. Matter* **2010**, *22*, 454112.
- (32) Liu, L.; Yang, C.; Zhao, K.; Li, J.; Wu, H.-C. Ultrashort Single-Walled Carbon Nanotubes in a Lipid Bilayer as a New Nanopore Sensor. *Nat. Commun.* **2013**, *4* (1), 2989.
- (33) Geng, J.; Kim, K.; Zhang, J.; Escalada, A.; Tunuguntla, R.; Comolli, L. R.; Allen, F. I.; Shnyrova, A. V.; Cho, K. R.; Munoz, D.; et al. Stochastic Transport Through Carbon Nanotubes in Lipid Bilayers and Live Cell Membranes. *Nature* **2014**, *514* (7524), 612–615.
- (34) Yang, F.; Wang, K.; Sun, D.; Zhao, W.; Wang, H.-Q.; He, X.; Wang, G.-R.; Bai, J.-T. Direct Observation of  $\lambda$ -DNA Molecule Reversal Movement within Microfluidic Channels under Electric Field with Single Molecule Imaging Technique. *Chin. Phys. B* **2016**, *25* (7), No. 078201.
- (35) van Dijk, M.; Bonvin, A. M. J. J. 3D-DART: a DNA Structure Modelling Server. *Nucleic Acids Res.* **2009**, *37*, W235.
- (36) Humphrey, W.; Dalke, A.; Schulten, K. VMD: Visual molecular dynamics. *J. Mol. Graphics* **1996**, *14* (1), 33–38.
- (37) Phillips, J. C.; Braun, R.; Wang, W.; Gumbart, J.; Tajkhorshid, E.; Villa, E.; Chipot, C.; Skeel, R. D.; Kalé, L.; Schulten, K. Scalable Molecular Dynamics with NAMD. *J. Comput. Chem.* **2005**, *26* (16), 1781–1802.
- (38) MacKerell, A. D.; Bashford, D.; Bellott, M.; Dunbrack, R. L.; Evanseck, J. D.; Field, M. J.; Fischer, S.; Gao, J.; Guo, H.; Ha, S.; et al. All-Atom Empirical Potential for Molecular Modeling and Dynamics Studies of Proteins. *J. Phys. Chem. B* **1998**, *102*, 3586–3616.
- (39) Yang, L.; Garde, S. Modeling the Selective Partitioning of Cations into Negatively Charged Nanopores in Water. *J. Chem. Phys.* **2007**, *126* (8), No. 084706.
- (40) Song, C.; Corry, B. Intrinsic Ion Selectivity of Narrow Hydrophobic Pores. *J. Phys. Chem. B* **2009**, *113* (21), 7642–7649.
- (41) Sahu, S.; Zwolak, M. Colloquium: Ionic Phenomena in Nanoscale Pores through 2D Materials. *Rev. Mod. Phys.* **2019**, *91* (2), 021004.
- (42) Wu, J.; Gerstandt, K.; Zhang, H.; Liu, J.; Hinds, B. J. Electrophoretically Induced Aqueous Flow through Single-Walled Carbon Nanotube Membranes. *Nat. Nanotechnol.* **2012**, *7* (2), 133–139.
- (43) Liu, H.; Jameson, C. J.; Murad, S. Molecular Dynamics Simulation of Ion Selectivity Process in Nanopores. *Mol. Simul.* **2008**, *34* (2), 169–175.
- (44) Leung, K.; Rempe, S. B.; von Lilienfeld, O. A. Ab Initio Molecular Dynamics Calculations of Ion Hydration Free Energies. *J. Chem. Phys.* **2009**, *130* (20), 204507.
- (45) Hummer, G.; Pratt, L. R.; García, A. E. Free Energy of Ionic Hydration. *J. Phys. Chem.* **1996**, *100* (4), 1206–1215.
- (46) Koneshan, S.; Rasaiah, J. C.; Lynden-Bell, R. M.; Lee, S. H. Solvent Structure, Dynamics, and Ion Mobility in Aqueous Solutions at 25 °C. *J. Phys. Chem. B* **1998**, *102* (21), 4193–4204.
- (47) Rasaiah, J. C.; Lynden-Bell, R. M. Computer Simulation Studies of the Structure and Dynamics of Ions and Non-Polar Solutes in Water. *Philos. Trans. R. Soc., A* **2001**, *359* (1785), 1545–1574.
- (48) Mancinelli, R.; Botti, A.; Bruni, F.; Ricci, M. A.; Soper, A. K. Hydration of Sodium, Potassium, and Chloride Ions in Solution and the Concept of Structure Maker/Breaker. *J. Phys. Chem. B* **2007**, *111* (48), 13570–13577.
- (49) Ma, J.; Li, K.; Li, Z.; Qiu, Y.; Si, W.; Ge, Y.; Sha, J.; Liu, L.; Xie, X.; Yi, H.; et al. Drastically Reduced Ion Mobility in a Nanopore Due to Enhanced Pairing and Collisions between Dehydrated Ions. *J. Am. Chem. Soc.* **2019**, *141* (10), 4264–4272.
- (50) Zheng, M.; Jagota, A.; Semke, E. D.; Diner, B. A.; Mclean, R. S.; Lustig, S. R.; Richardson, R. E.; Tassi, N. G. DNA-Assisted Dispersion and Separation of Carbon Nanotubes. *Nat. Mater.* **2003**, *2* (5), 338–342.
- (51) Zhao; Johnson, J. K. Simulation of Adsorption of DNA on Carbon Nanotubes. *J. Am. Chem. Soc.* **2007**, *129* (34), 10438–10445.
- (52) Kowalczyk, S. W.; Wells, D. B.; Aksimentiev, A.; Dekker, C. Slowing down DNA Translocation Through a Nanopore in Lithium Chloride. *Nano Lett.* **2012**, *12* (2), 1038–1044.
- (53) Wilson, J.; Aksimentiev, A. Water-Compression Gating of Nanopore Transport. *Phys. Rev. Lett.* **2018**, *120* (26), 268101.
- (54) Hummer, G. Water, Proton, and Ion Transport: from Nanotubes to Proteins. *Mol. Phys.* **2007**, *105* (2–3), 201–207.
- (55) Steinbock, L. J.; Radenovic, A. The Emergence of Nanopores in next-Generation Sequencing. *Nanotechnology* **2015**, *26* (7), No. 074003.